

See discussions, stats, and author profiles for this publication at: <https://www.researchgate.net/publication/14257814>

# Biochemical and spectroscopic properties of the four-subunit quinol oxidase (cytochrome ba(3)) from *Paracoccus denitrificans*

ARTICLE *in* BIOCHIMICA ET BIOPHYSICA ACTA · DECEMBER 1996

Impact Factor: 4.66 · DOI: 10.1016/S0005-2728(96)00086-2 · Source: PubMed

---

CITATIONS

23

---

READS

17

6 AUTHORS, INCLUDING:



[Stefan Anemüller](#)

Universität zu Lübeck

64 PUBLICATIONS 1,180 CITATIONS

SEE PROFILE

## Biochemical and spectroscopic properties of the four-subunit quinol oxidase (cytochrome *ba*<sub>3</sub>) from *Paracoccus denitrificans*

Irmela Zickermann<sup>a</sup>, Stefan Anemüller<sup>b</sup>, Oliver-Matthias H. Richter<sup>a</sup>, Oltea S. Tautu<sup>c</sup>,  
Thomas A. Link<sup>c</sup>, Bernd Ludwig<sup>a,\*</sup>

<sup>a</sup> Institute of Biochemistry / Molecular Genetics, University of Frankfurt, Biozentrum N200, Marie-Curie-Str. 9, D-60439 Frankfurt, Germany

<sup>b</sup> Institute of Biochemistry, Medical University of Lübeck, Ratzeburger Allee 160, D-23538 Lübeck, Germany

<sup>c</sup> Zentrum der Biologischen Chemie, Klinikum der J.W. Goethe Universität Frankfurt, D-60590 Frankfurt, Germany

Received 29 April 1996; revised 24 June 1996; accepted 2 July 1996

### Abstract

The *ba*<sub>3</sub> quinol oxidase from *Paracoccus denitrificans* has been purified by a new protocol leading to significantly higher yields than previously reported (Richter et al. (1994) J. Biol. Chem. 269, 23079–23086). In an SDS PAG an additional protein band compared with the previous preparation appears, which can be identified as the major form of subunit II. All protein bands can be assigned to genes of the *qox* operon by N-terminal sequencing, indicating that the oxidase consists of four subunits. In addition to one heme A, one heme B, and one copper atom, the preparation contains two ubiquinone molecules per enzyme. The oxidase is further characterized by electron paramagnetic resonance (EPR), circular dichroism (CD) and magnetic circular dichroism (MCD) spectroscopy.

**Keywords:** Heme-copper oxidase; *Qox* operon; Circular dichroism; Magnetic circular dichroism; Lipoprotein; (*Thermus thermophilus*)

### 1. Introduction

*Paracoccus denitrificans* is a gram-negative soil bacterium, which expresses three different terminal oxidases [1]. Two cytochrome-*c* oxidases, one of the cytochrome *aa*<sub>3</sub>-type and one of the cytochrome *cbb*<sub>3</sub>-type have been described. A further branching point in the respiratory chain is found at the level of

ubiquinone. Both cytochrome-*c* oxidases and the quinol oxidase belong to the heme-copper oxidases. Members of this family are characterized by a binuclear centre in subunit I consisting of a high-spin heme and a Cu<sub>B</sub> site, where oxygen reduction takes place [2–5]. Moreover, a second heme component is found in the same subunit. All heme-copper oxidases pump protons against an electrochemical gradient across the membrane to generate a proton motive force.

Heme-copper oxidases can be divided into two groups according to their electron donor, which is in one case the one-electron carrier cytochrome *c*, in the other case the two-electron carrier ubiquinol. Structurally these two classes differ in subunit II. Cy-

Abbreviations: PAG(E), polyacrylamide gel (electrophoresis); CD, circular dichroism; MCD, magnetic circular dichroism; TXRF, total reflection X-ray fluorescence; EPR, electron paramagnetic resonance; IMAC, immobilized metal affinity chromatography.

\* Corresponding author. Fax: +49 69 79829244; e-mail: ludwig@em.uni-frankfurt.d400.de.

tochrome-*c* oxidases contain a further metal centre in this subunit, which is a binuclear  $\text{Cu}_A$  site in *aa\_3*-type oxidases, whereas *cbb\_3*-type oxidases contain two additional subunits carrying *c*-type hemes. Quinol oxidases lack any metal centre in subunit II, so that these enzymes only accommodate three redox-active metal ions. The oxygen reduction mechanism of both types of enzyme is believed to be identical [6]. In the *bo\_3* quinol oxidase from *E. coli* bound ubiquinone was detected [7,8] which may play the role of the  $\text{Cu}_A$  in cytochrome-*c* oxidases. However, no other quinol oxidase has so far been shown to contain bound quinones.

The cytochrome *ba\_3* quinol oxidase from *P. denitrificans* has been purified and shown to contain an *a*-type heme in its high-spin site and a *b*-type heme in its low-spin site [9,10]. The yield of the previous, time-consuming purification was only 5% based on enzymatic activity, although an overproducing strain was used. In a SDS PAG five protein bands were detected, but only four genes organized in an operon-like structure (*qoxABCD*) were found by DNA sequencing. The appearance of the fifth protein band in the SDS PAG could not be explained.

Here we present a new purification protocol and further characterization of the *ba\_3* quinol oxidase from *P. denitrificans*. In the preparation a major form of subunit II appears in the SDS PAG. The identity of all four gene products of the *qox* operon is now confirmed by N-terminal sequencing of the subunits of the quinol oxidase. Evidence for a further electron carrier besides heme A, heme B and the  $\text{Cu}_B$  is presented. The spectroscopic characterization includes EPR, CD and MCD spectra of the purified quinol oxidase.

## 2. Materials and methods

### 2.1. Strain and growth condition

*Paracoccus denitrificans* strain G440 (deletion mutant in the *fbc* operon coding for the cytochrome *bc\_1* complex,  $\Delta fbc::neo$ ) was grown on succinate medium [11]. For site-directed mutagenesis experiments use was made of *P. denitrificans* ORI 2/4, which is deleted in the *qox* operon and no expression of any quinol oxidase is observed. This strain was

complemented with a broad host-range plasmid [11] carrying the mutated *qox* operon. The strain was grown as described above except that streptomycin sulfate (25  $\mu\text{g}/\text{ml}$ ) was added to the growth medium. Cells were disrupted and membranes isolated as described previously [12].

### 2.2. Activity assay

Enzymatic activity of the solubilized fraction was measured at room temperature in a Kontron Uvikon 941 at 275 nm in 50 mM  $\text{KP}_i$  (pH 7.5), 1 mM EDTA, 5 g/l dodecyl ethoxysulfate [10] and 50  $\mu\text{M}$  of the decyl analog of ubiquinol (Sigma) ( $\Delta\epsilon_{\text{ox-red, 275nm}} = 12.5 \text{ mM}^{-1}\text{cm}^{-1}$ ).

### 2.3. Isolation of the *ba\_3* quinol oxidase

All steps were performed at 4°C. Membranes were solubilized in the presence of 1.5 g *n*-dodecyl- $\beta$ -D-maltoside per 1 g membrane protein in 50 mM  $\text{KP}_i$  (pH 7.0), 1 mM EDTA, 50 mM NaCl and 50  $\mu\text{M}$  Pefabloc SC (Biomol, Hamburg). After centrifugation at  $100\,000 \times g$ , the supernatant was loaded onto a Q-Sepharose Fast Flow column (Pharmacia), equilibrated with a buffer containing 20 mM  $\text{KP}_i$  (pH 7), 100 mM NaCl and 0.5 g/l dodecyl maltoside. The elution was done with five column volumes of a linear salt gradient from 100–500 mM NaCl in equilibration buffer. Pooled fractions were applied to an immobilized metal affinity chromatography column (IMAC, Fast Flow Sepharose, Pharmacia), loaded with copper and equilibrated with 20 mM  $\text{KP}_i$  (pH 7.0), 150 mM NaCl, 0.5 g/l dodecyl maltoside. A linear gradient of five column volumes containing 0 to 100 mM imidazole in the equilibration buffer and one volume of the buffer with the final imidazole concentration was used for elution of the column. Fractions with the highest specific enzymatic activity were concentrated 20-fold and chromatographed on a gel filtration column (Ultrogel AcA 34, Serva) equilibrated with 20 mM  $\text{KP}_i$  (pH 7), 100 mM NaCl, 1 mM EDTA and 0.2 g/l dodecyl maltoside. Fractions were pooled according to enzymatic activity and SDS PAG, concentrated and stored at  $-80^\circ\text{C}$ . Protein determination and SDS PAGE were performed as described elsewhere [13–15].

For the experiment including protease inhibitors,

the following concentrations were used for cell disruption: aprotinin, 74  $\mu\text{M}$ ; E 64, 1.4  $\mu\text{M}$ ; pepstatin, 1  $\mu\text{M}$ ; Pefabloc SC, 0.4 mM, phosphoramidon, 7  $\mu\text{M}$ ; leupeptin, 1  $\mu\text{M}$  (all Boehringer, Mannheim). Phosphoramidon and leupeptin were also used in the subsequent purification steps in the same concentrations.

#### 2.4. Site-directed mutagenesis

Site-directed mutagenesis was done according to the 'altered sites' mutagenesis protocol (Promega, Heidelberg).

#### 2.5. N-terminal sequencing

1 mg of purified *ba*<sub>3</sub> quinol oxidase was electrophoresed on a Tricine SDS gel [15], blotted onto a polyvinylidene difluoride membrane and stained with Coomassie-Blue G 250 (Serva, Heidelberg) in 25% methanol, 10% acetic acid. All major protein bands were directly submitted to N-terminal sequencing with an Applied Biosystems 473A sequencer (Weiterstadt) with an on-line phenylthiohydantoin detector.

#### 2.6. Metal and phosphorus analysis

The copper content of the protein complex was measured by atomic absorption with the graphite tube technique on a Perkin Elmer AAS 2380. A simultaneous determination of copper, iron, phosphorus and sulfur content was done by total reflection X-ray fluorescence analysis [16]. The sample buffer was 100 mM Tris/acetate (pH 8), 1 mM EDTA, 0.2 g/l dodecyl maltoside.

#### 2.7. Quinone extraction

Bound quinone molecules of the purified *ba*<sub>3</sub> quinol oxidase were extracted with chloroform/ethanol as described in Ref. [17] or with a mixture of methanol and light petroleum as described in Ref. [18]. Difference spectra were recorded in 80% ethanol 20% 50 mM  $\text{KP}_i$  (pH 7.5) and the extinction coefficient (272 nm) of 12.5  $\text{mM}^{-1} \text{cm}^{-1}$  was used to determine the concentration.

#### 2.8. Spectroscopy

Optical spectra were recorded on a Bruins Omega 10 spectrometer, separation of individual heme spectra was done according to Ref. [19]. For quantitation of the heme *b* content a  $\Delta\epsilon_{\text{red-ox}, 563\text{nm}} = 18 \text{ mM}^{-1} \text{cm}^{-1}$  was used. EPR spectra were measured on a Bruker ER 200 cw spectrometer. CD and MCD spectra were recorded on a CD-spectropolarimeter Jasco J-720 with an additional equipment for MCD spectroscopy.

### 3. Results and discussion

#### 3.1. Purification

The *ba*<sub>3</sub> quinol oxidase from *Paracoccus denitrificans* has previously been purified and optical spectra have been recorded [9,10]. Here we report a new purification scheme with significantly higher yields compared with the one of Richter et al. [10].

The new protocol involves three chromatographic steps including (1) ion exchange, (2) immobilized metal affinity chromatography (IMAC) with copper as metal ion and (3) gel filtration. Especially IMAC leads to an almost pure enzyme complex (Fig. 1A). The subsequent gel filtration step is necessary to eliminate the imidazol which is used in the elution buffer of the IMAC. Imidazole is able to complex heme components and may disturb the characteristic spectral properties of the hemes. Very recently good purification results with three other bacterial terminal oxidases of the heme-copper family have been achieved, when IMAC was used as a chromatographic technique [20]. Especially histidine and tryptophane residues are known to exhibit a high affinity to the IMAC material [21], a surface property obviously shared by several of the terminal oxidases as well.

When column fractions were analyzed for enzymatic activity, no evidence for a second quinol oxidase expressed under this growth condition was found. Investigations of membranes from quinol oxidase deletion strains confirm this result [1].

The yield of the new purification scheme is about 30% based on enzymatic activity (Table 1), which is significantly higher than 5% which was achieved by

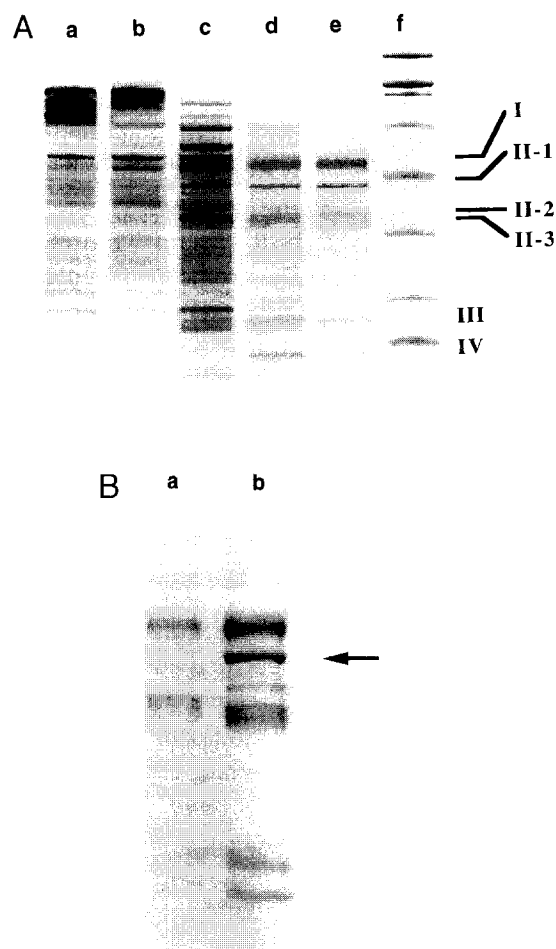


Fig. 1. Purification of the quinol oxidase from *P. denitrificans*. (A) Separation on a 10% Tricine SDS gel of fractions obtained during the purification according to Table 1. (a) 50  $\mu$ g membranes of strain G440 (b) 40  $\mu$ g of solubilized protein (c) 20  $\mu$ g after Q-Sepharose (d) 10  $\mu$ g after IMAC (e) 6  $\mu$ g after gel filtration (f) molecular weight standards: myosin 200 kDa,  $\beta$ -galactosidase 116.250 kDa, phosphorylase b 97.4 kDa, serum albumin 66.2 kDa, ovalbumin 45 kDa, carbonic anhydrase 31 kDa, trypsin inhibitor 21.5 kDa, lysozyme 14.4 kDa, aprotinin 6.5 kDa. (B) Comparison of the preparation of Richter et al. ([10]; lane a) and the new preparation (lane b) on a 12% SDS gel. The arrow indicates the additional protein band in the new preparation.

the method of Richter et al. [10]. The spectral properties of the new preparation are in accordance with those of the one previously reported, concerning reduced minus oxidized, pyridine hemochrome and CO spectra (data not shown). Since we switched to a commercially available quinol analog as substrate in the enzyme assay, activities of both preparations are not directly comparable, but the purification factor based on enzymatic activity is in the same range.

The *qox* operon codes for four proteins; however, five protein bands appeared in the SDS PAG of the previous preparation. Peptide sequence information could only be obtained from subunit II, while the other subunits were assigned to the genes only based on their size [10]. Here we identify all protein bands by N-terminal sequencing, which all show predicted amino acid sequences from the *qox* operon (Table 2). Only subunit II is translated with a signal sequence, which is later processed, while the other subunits start with the predicted amino acid following the methionine. Subunit IV starts with the third predicted amino acid. N-terminal processing of subunit II seems to be common and is observed in the quinol oxidases from *Acetobacter aceti*, *Bacillus subtilis* and the cytochrome *c* oxidase from *P. denitrificans* [22–24]. The most likely explanation is that a signal sequence is needed for translocation of the large periplasmic domain across the membrane.

Comparison of the two preparations on an SDS gel (Fig. 1B) shows that the new preparation contains an additional protein band, which is identified as a form of subunit II with the highest  $M_r$ . The  $M_r$  of the new form of subunit II as judged from SDS PAG is 43500, being close to 41966 calculated from the DNA-derived amino acid sequence. Other apparently shorter forms, which seem to be similar to subunit II of the previous preparation, do not stain as intensively as the large form. The same staining pattern is observed when the preparation of membranes and the purification steps are performed in the presence of a set of protease inhibitors (see Section 2). The N-termini of all forms exhibit the same amino acid sequence.

### 3.2. N-terminal processing of subunit II

Richter et al. [10] speculated that the N-terminal cysteine residue of subunit II of the *ba<sub>3</sub>* quinol oxidase from *P. denitrificans* may be modified by fatty acids, because a consensus sequence found at the processing sites of *E. coli* lipoproteins is present in this subunit as well. In lipoproteins, however, N-terminal processing is preceded by cysteine modification [25]. Those modifications are also observed in an integral membrane protein from a phylogenetically related organism [26]. We mutated the N-terminal cysteine to alanine, thus excluding any possibility

Table 1

Purification of the *ba*<sub>3</sub> quinol oxidase from membranes of *P. denitrificans* strain G440

Material	Protein [mg]	Activity		Yield <sup>(1)</sup> [%]	Purification factor
		[U]	[U/mg]		
Isolated membranes	1200	n.d.	n.d.		
Supernatant after detergent extraction	661	1115	1.7	100	1
Ion-exchange chromatography	150	988	6.6	88	3.9
Metal affinity chromatography	19	777	43	70	25
Gel filtration	6.7	374	55	33	32

<sup>(1)</sup> Yield based on specific activity; for details see Sections 2.2 and 3.

of a fatty acid modification at this position. Analyses of an SDS PAG of the purified enzyme indicated no inhibition of the processing step, so that we conclude that none of the different forms of subunit II found in the wild-type enzyme is caused by unusual migration behaviour due to modifications with different fatty acids. It is interesting to note that a similar mutation in the *bo*<sub>3</sub> oxidase from *E. coli*, where a comparable consensus sequence is found, lead to the unprocessed protein (Gennis, R.B., personal communication).

Most likely the three forms of subunit II differ in their C-termini. The *aa*<sub>3</sub> cytochrome-*c* oxidase from *Rhodobacter sphaeroides* exhibits different forms of

subunit II as well, which could be separated chromatographically [20]. Subunit II of the quinol oxidase from *P. denitrificans* was shown by DNA sequencing to be significantly larger compared with other quinol oxidases [10]. One may speculate that the shorter forms are due to the cleavage of this extension by a protease not affected by the set of protease inhibitors used.

### 3.3. Metal analysis

We assayed the copper content by two independent methods: (1) determination by atomic absorption spectroscopy yielded a ratio between 0.9 and 1.3 copper per heme *b*, determined spectroscopically. (2) Alternatively TXRF (total reflection X-ray fluorescence) analysis is used to simultaneously determine the copper, iron and sulfur content. The sulfur value is used to estimate the protein amount based on the sum of methionine and cysteine content calculated from the protein sequence. Table 3 summarizes the results when the quinol oxidase concentration is calculated by (A) the sulfur content or by (B) dividing the sum of the iron and copper content by three. The almost identical oxidase concentrations derived by method A and B are taken as more evidence for the purity of the preparation. The results are indicative of a stoichiometry of two iron atoms and one copper atom per enzyme complex. The two iron atoms can be assigned to the two hemes. The value of one copper per complex is in agreement with the fact that quinol oxidases of the heme-copper family do not comprise a Cu<sub>A</sub> centre as can be shown by the lack of the ligands for this centre in subunits II of the quinol oxidases, but only contain Cu<sub>B</sub> in the binuclear centre.

Table 2

Alignment of the N-terminal peptide sequence of the mature subunits with DNA-derived protein sequence of the gene products, and their *M<sub>r</sub>*

subunit / gene product	N-terminal sequence	<i>M<sub>r</sub></i>
I	ATFSNETT	51000 <sup>1</sup>
QoxB	MATFSNETT	75072 <sup>2</sup>
II-1	xxAEVLAP	43500 <sup>1</sup>
II-2	xKAEV	37000 <sup>1</sup>
II-3	xKAEV	34000 <sup>1</sup>
QoxA	(aa) 18-LAACKAEVLAP	41966 <sup>2</sup>
III	WHATTDXM	17500 <sup>1</sup>
QoxC	MSHATTDTM	22907 <sup>2</sup>
IV	AEHAHAH	14000 <sup>1</sup>
QoxD	MSAEHAHAH	13959 <sup>2</sup>

<sup>(1)</sup> judged from SDS PAG; <sup>(2)</sup> deduced from DNA sequence; for calculating the *M<sub>r</sub>* of QoxA, the second possible start codon was used. II-1, II-2 and II-3 refer to three different forms of subunit II. (aa) amino acid; x, no amino acid identified in this cycle. A discrepancy in the first sequencing cycle of subunit III is noted.

Table 3

Metal content of the  $ba_3$  quinol oxidase from *P. denitrificans* measured by total reflection X-ray fluorescence [16]

A <sup>(a)</sup>				B <sup>(b)</sup>		
Fe:Cu ratio	Oxidase [nmol/ml]	Cu:Ox ratio	Fe:Ox ratio	Oxidase [nmol/ml]	Cu:Ox ratio	Fe:Ox ratio
2.1	23.4	1.08	2.24	25.7	0.97	2.03

The calculation is based on <sup>(a)</sup> the sulfur content, <sup>(b)</sup> the sum of iron and copper content divided by three.

### 3.4. Quinone extraction

Quinone was extracted by two different methods. The extracts were analyzed by difference spectra (air-oxidized minus borohydride-reduced) in the UV region. Independently of the extraction methods the absorption maximum is at 272 nm which is typical for isolated quinones measured in the buffer used. The line-shape of the (ox-red) spectrum shows no evidence for the presence of menaquinone, but clearly demonstrates that ubiquinone is extracted from the quinol oxidase. This is in agreement with the fact that bacteria from the  $\alpha$ -subdivision of non-sulfur purple bacteria, to which *P. denitrificans* belongs, contain ubiquinone-10 in their membranes [27]. By quantitating the quinone content in relation to the heme *b* content of the oxidase, ratios between 2.2 to 2.5 quinones per heme *b* were obtained. The same methods applied to the  $aa_3$  cytochrome-*c* oxidase from *P. denitrificans* yielded a ratio of 0.3 quinones per complex. Quinone is a lipophilic molecule which may be bound unspecifically to contaminating phospholipids of the preparation. The phospholipid content can be estimated by the measurement of phosphorus by TXRF. The cytochrome  $ba_3$  quinol oxidase contains 25 phospholipids,  $aa_3$  cytochrome-*c* oxidase 12 phospholipids. Therefore it is very unlikely that the difference in the quinone content is due to a different phospholipid content.

It has already been shown that the  $bo_3$  quinol oxidase from *E. coli* contains quinones [7]. Depending on sample preparation, 1.0–2.2 quinone molecules were found in this oxidase. Using mutants unable to synthesize ubiquinone, the authors showed that besides the substrate binding site ( $Q_L$ , most likely in subunit II [28]), another quinone binding site exists, which binds quinone much more tightly ( $Q_H$ ). One

could speculate that the two quinones which are reproducibly found in the  $ba_3$  quinol oxidase from *P. denitrificans* are bound to equivalents of the  $Q_H$  and  $Q_L$  sites in the *E. coli* oxidase and that these sites are a general feature of quinol oxidases. If, in addition to the two hemes and the  $Cu_B$ , the quinone in the  $Q_H$  site is redox-active, it may function as an analog to  $Cu_A$  found in cytochrome-*c* oxidases. The quinone in the  $Q_L$  site would then be an equivalent to the mobile electron carrier cytochrome *c*. Ingledew et al. [8] analysed the hyperfine structure in an EPR spectrum of a highly stabilized semiquinone in the  $bo_3$  oxidase from *E. coli*. They suggest that the splitting of the signal may be due to a second semiquinone in a distance of approx. 1.5 nm. Evidence for a role of one quinone molecule in the enzymatic mechanism is shown by kinetic measurements. A preparation of the  $bo_3$  oxidase from *E. coli* containing one quinone molecule, was shown to exhibit multiphasic kinetics comparable to cytochrome-*c* oxidases when analysed by flow flash and stopped flow techniques. However, monophasic kinetics are observed, when the quinone molecule is absent from the enzyme [29].

### 3.5. EPR spectroscopy

The  $ba_3$  quinol oxidase was further characterized by EPR spectroscopy. The EPR spectrum (Fig. 2) clearly shows the presence of one low-spin and one high-spin heme component in the enzyme. The high-spin heme signal could be simulated with the following *g*-values and line-widths (given in parenthesis):  $g_y = 6.03$  (7 mT),  $g_x = 5.97$  (4 mT) and  $g_z = 2.00$  (10 mT). The *g*-values of the high-spin heme are typical for a nearly axial centre (rhombicity:  $E/D < 0.002$ ). The low-spin heme signal could be simulated with the following *g*-values and line-widths:  $g_z = 2.98$  (3 mT),  $g_y = 2.247$  (3.3 mT) and  $g_x = 1.495$  (16.5 mT). The *g*-values as well as the crystal field parameters of the low-spin heme (tetragonal field:  $\Delta/\lambda = 3.34$ , rhombicity:  $V/\lambda = 1.799$ ) are very similar to those of the mitochondrial cytochrome-*c* oxidase and the cytochrome  $bo_3$  from *E. coli*, indicating a bis-histidyl ligation of the low-spin heme centre [30]. The two histidine residues which ligate the low-spin heme in the  $aa_3$  cytochrome *c* oxidase from *P. denitrificans* as shown by the crystal structure

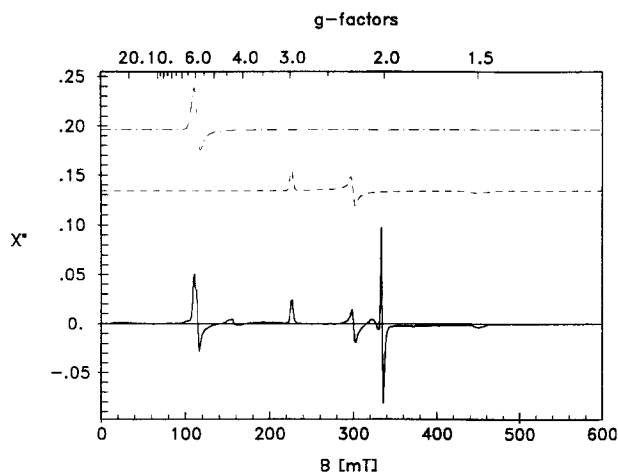


Fig. 2. EPR spectrum of the  $ba_3$  quinol oxidase from *P. denitrificans*. Solid line: Spectrum of the quinol oxidase. Protein concentration was 30  $\mu$ M in 20 mM  $KP_i$  (pH 8), 100 mM NaCl, 1 mM EDTA and 0.2 g/l dodecyl maltoside. Recording conditions were 20.0 K, microwave power 20.0 mW, microwave frequency 9.431 GHz, modulation amplitude 20 G. Upper dotted line: simulation of the high-spin heme. Lower dotted line: simulation of the low-spin heme.

[31], are also conserved in quinol oxidases. Resonances characteristic for  $Cu_A$  and manganese, which are typically observed in the EPR spectra of cytochrome-*c* oxidase from *P. denitrificans* [32], are obviously absent in the spectrum. This is in agreement with the metal determinations, which yielded a copper stoichiometry of one copper per complex, thus identifying the copper as the EPR invisible  $Cu_B$  atom of the binuclear centre. In the  $g = 2$  region an additional resonance is observed, which, due to its relaxation behaviour, can be identified as an iron-sulfur centre, probably of the  $[3Fe4S]$  type. However, since the double integral of the resonances has to be considered for the spin determination, it is obvious that the oxidase preparation contains only minor amounts of this contaminant. This is confirmed by the metal analysis (see above) where no significantly elevated iron content could be detected.

EPR spectra of wild-type membranes from *P. denitrificans* were already recorded by Haltia et al. [33]. Besides the prominent  $g_z = 2.89$  signal of  $aa_3$  cytochrome-*c* oxidase, a second peak maximum of significantly lower intensity was found at  $g = 2.97$ . When mutants of subunit III of the cytochrome-*c* oxidase were recorded, an elevated level of the  $g = 2.97$  signal was measured. As already speculated by

Haltia et al., we confirm here that this signal originates from the  $ba_3$  quinol oxidase.

### 3.6. Optical spectroscopy

The absolute spectra of the  $ba_3$  quinol oxidase are shown in Fig. 3, upper panel. The oxidised form has the maximum of the Soret band at 417 nm; the reduced form shows a maximum at 429 nm with a shoulder at approx. 440 nm which can be assigned to the contribution of the heme  $a_3$ . In the (reduced minus oxidised) spectrum, the signals of heme *a* and *b* in the  $\alpha$ -region are well separated with maxima at 563 and 609 nm while the signals overlap in the Soret region. Fig. 3, lower panel, shows the (reduced minus oxidised) spectrum of the individual heme components after separation according to the method

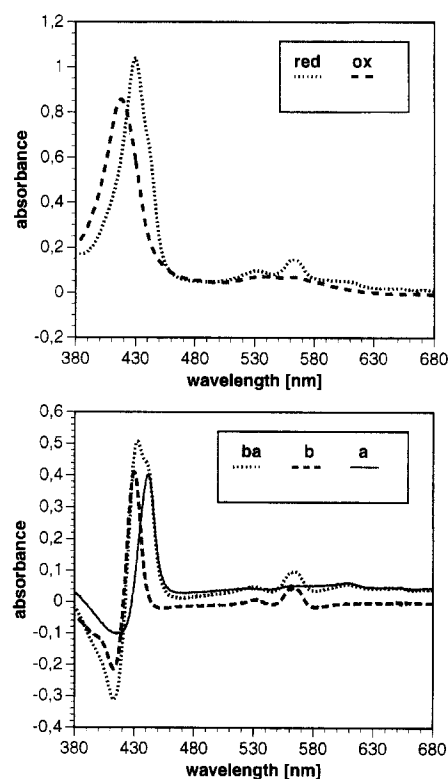


Fig. 3. Absorption spectra of the  $ba_3$  quinol oxidase from *P. denitrificans*. (Upper panel) Absolute spectra of the air-oxidized and dithionite-reduced enzyme. (Lower panel) (Reduced minus oxidized) spectrum of the  $ba_3$  enzyme and spectra calculated for the individual hemes by the method of Vanneste [19]. Oxidase concentration was 8  $\mu$ M in 20 mM  $KP_i$  (pH 8), 100 mM NaCl, 1 mM EDTA and 0.2 g/l dodecyl maltoside, light path 5 mm.



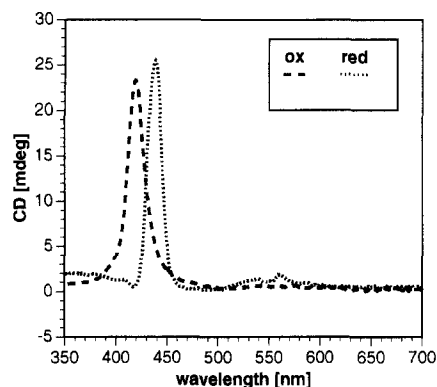


Fig. 4. CD spectra of the  $ba_3$  quinol oxidase from *P. denitrificans*. Absolute spectra of the air-oxidized and dithionite-reduced enzyme. Oxidase concentration was 8  $\mu$ M in 20 mM  $KP_i$  (pH 8), 100 mM NaCl, 1 mM EDTA and 0.2 g/l dodecyl maltoside, light path 5 mm.

of Vanneste [19]. The maximum of heme *b* in the Soret region is at 430 nm and that of heme *a* at 442 nm. The absorption spectra of the individual heme species are another confirmation that the quinol oxidase from *P. denitrificans* does not contain heme *b* in its high-spin site, as has been proposed by de Gier et al. [1]. These authors suggested that the heme composition varies due to different strain backgrounds. However, we also find heme *a* in the high-spin site in a strain where the  $bc_1$  complex is not deleted (Zickermann, I., unpublished).

### 3.7. Circular dichroism spectroscopy

The CD spectrum of the  $ba_3$  quinol oxidase in the Soret region is dominated by a strong positive band around 419 nm in the oxidised state and around 438

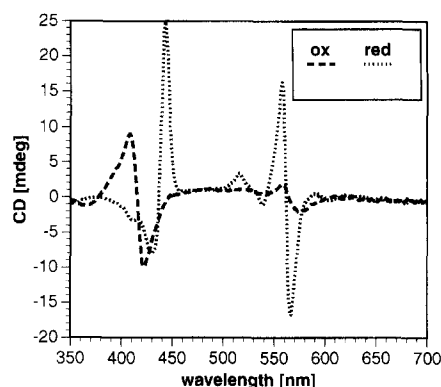


Fig. 5. MCD spectra of the  $ba_3$  quinol oxidase from *P. denitrificans*. Absolute spectra of the air-oxidized and dithionite-reduced enzyme. Oxidase concentration was 8  $\mu$ M in 20 mM  $KP_i$  (pH 8), 100 mM NaCl, 1 mM EDTA and 0.2 g/l dodecyl maltoside, light path 5 mm. The spectra were recorded at room temperature,  $H = 0.86$  T.

nm in the reduced state (Fig. 4). The spectra are very similar to the CD spectra of  $aa_3$  cytochrome-*c* oxidases [34]. This shows that the CD spectra are predominantly due to contributions of the  $a_3$  heme. This conclusion was confirmed by the analysis of the (reduced-oxidised) CD spectra of the individual hemes (not shown). In the CD spectra, there is no indication for an interaction between the transitions of both hemes.

### 3.8. Magnetic circular dichroism spectroscopy

MCD spectra of hemes are sensitive to the redox and spin state of the central iron atom [35]. Fig. 5 shows the MCD spectra of air-oxidised and dithionite-reduced  $ba_3$  quinol oxidase. The spectrum of the

Table 4

Comparison of the MCD characteristics of the  $ba_3$  quinol oxidase from *P. denitrificans* and the  $ba_3$  cytochrome-*c* oxidase from *Thermus thermophilus* [37]

Redox status	$ba_3$ quinol oxidase		$ba_3$ cytochrome- <i>c</i> oxidase	
	band extrema [nm]	$\Delta\epsilon/H$ [ $M^{-1}cm^{-1}T^{-1}$ ]	band extrema [nm]	$\Delta\epsilon/H$ [ $M^{-1}cm^{-1}T^{-1}$ ]
Oxidised	408	80	405	42
	422.5	−87	421	−63
	558	16	555	22
	573	−17	577	−13
Reduced	429.5	−70	432	−35
	443	219	445	117
	557.5	144	556	120
	566	−148	564	−134

oxidised form shows pseudo-A-terms centred at 415.5 nm and 564 nm. These bands are characteristic for oxidised low-spin hemes and are similar to those found in other oxidised low-spin hemes, e.g., ferri-cytochrome *c* or ferri-cytochrome *b<sub>5</sub>*. Oxidised high-spin hemes show only very weak MCD signals.

The MCD spectrum of the reduced form shows a strong MCD-A-term centred at 561.5 nm and a positive C-term at 443 nm. The A-term in the  $\alpha$ -region belongs to the *Q<sub>0</sub>* band of reduced heme *b* and clearly shows that heme *b* is in the low-spin state. The C-term at 443 nm belongs to the high-spin heme *a<sub>3</sub>* and is again very similar to the signal observed in *aa<sub>3</sub>* cytochrome-*c* oxidases [36]. Thus, the MCD spectra provide clear evidence for the presence of both a low-spin heme *b* and a high-spin heme *a<sub>3</sub>*, in agreement with the conclusion of Richter et al. [10].

Goldbeck et al. [37] have reported MCD spectra of the *ba<sub>3</sub>* cytochrome-*c* oxidase from *Thermus thermophilus*. The MCD bands of both *ba<sub>3</sub>* oxidases are compared in Table 4. Although both enzymes use different electron donors, their oxidised and reduced spectra show very similar band positions and intensities. This is another confirmation of the close relationship of cytochrome-*c* oxidases and quinol oxidases from the heme-copper family.

#### 4. Conclusion

The *ba<sub>3</sub>* quinol oxidase from *P. denitrificans* was purified by a new protocol leading to significantly higher yields compared to the previously described protocol. The quinol oxidase contains two bound quinol molecules. EPR, CD, and MCD spectra confirm that the oxidase is a member of the heme-copper family of terminal oxidases. The different chemical nature of the low-spin heme (heme *b* vs. *a*) allows one to observe both hemes separately in the  $\alpha$ -region but does not have any obvious functional consequences. A further advantage of the *ba<sub>3</sub>* enzyme is that MCD spectra of *b*- or *c*-type hemes with a protoporphyrin IX-type ring system are far better understood than those of *a*-type hemes. Thus, the *ba<sub>3</sub>* quinol oxidase appears to be optimally suited for kinetic and spectroscopic studies.

#### Acknowledgements

We thank Herrmann Schägger for N-terminal sequencing, Axel Wittershagen for metal determinations by total reflection X-ray fluorescence, Miguel Teixeira for cooperation in EPR spectroscopy, and Oliver Hatzfeld for help with optical spectroscopy. Dodecyl ethoxysulfate was kindly provided by Henkel AG (Düsseldorf). The technical assistance of Inge Pecher is gratefully acknowledged as well as the atomic absorption measurements performed by Doris Bergmann-Dörr. We thank Volker Zickermann for critical discussions. This work was supported by Deutsche Forschungsgemeinschaft (SFB 169 and Li 474/2 to T.A.L.), Graduiertenkolleg 'Proteinstrukturen, Dynamik und Funktion', and Fonds der Chemischen Industrie.

#### References

- [1] De Gier, J.-W.L., Lübben, M., Reijnders, W.N.M., Tipker, C.A., Slotboom, D.-J., Van Spanning, R.J.M., Stouthamer, A.H. and Van der Oost, J. (1994) Mol. Microbiol. 13, 183–196.
- [2] Saraste, M., Holm, L., Lemieux, L., Lübben, M. and Van der Oost, J. (1991) Biochem. Soc. Trans. 19, 608–612.
- [3] Calhoun, M.W., Thomas, J.W. and Gennis, R.B. (1994) Trends Biochem. Sci. 19, 325–330.
- [4] Trumpower, B.L. and Gennis R.B. (1994) Annu. Rev. Biochem. 63, 675–716.
- [5] Van der Oost, J., De Boer, A.P.N., De Gier, J.-W.L., Zumft, W.G., Stouthamer, A.H. and Van Spanning, R.J.M. (1994) FEMS Microbiol. Lett. 121, 1–9.
- [6] Babcock, G.T. and Wikström, M. (1992) Nature 356, 301–309.
- [7] Sato-Watanabe, M., Mogi, T., Ogura, T., Kitagawa, T., Miyoshi, H., Iwamura, H. and Anraku, Y. (1994) J. Biol. Chem. 269, 28908–28912.
- [8] Ingledew, W.J., Ohnishi, T. and Salerno, J.C. (1995) Eur. J. Biochem. 227, 903–908.
- [9] Ludwig, B. (1992) Biochim. Biophys. Acta 1101, 195–197.
- [10] Richter, O.M.H., Tao, J., Turba, A. and Ludwig, B. (1994) J. Biol. Chem. 269, 23079–23086.
- [11] Gerhus, E., Steinrücke, P. and Ludwig, B. (1990) J. Bacteriol. 172, 2392–2400.
- [12] Ludwig, B. (1986) Methods Enzymol. 126, 153–159.
- [13] Lowry, O.H., Rosebrough, N.J., Farr, A.L. and Randall, R.J. (1951) J. Biol. Chem. 193, 265–275.
- [14] Markwell, M.A.K., Haas, S.M., Bieber, L. and Tolbert, N.E. (1978) Anal. Biochem. 87, 206–210.

- [15] Schägger, H. and von Jagow, G. (1987) *Anal. Biochem.* 166, 368–379.
- [16] Wittershagen, A., Rostam-Khani, P., Rittmeyer, C., Bublak, D., Stahl, G., Rüterjans, H. and Kolbesen, B.O. (1996) CANAS (Conference Abstract, Konstanz, 1995).
- [17] Ohnishi, T. and Trumpower, B.L. (1980) *J. Biol. Chem.* 255, 3278–3284.
- [18] Kröger, A. (1978) *Methods Enzymol.* 53D, 579–591.
- [19] Vanneste, W.H. (1966) *Biochemistry* 5, 838–848.
- [20] Warne, A., Wang, D.N. and Saraste, M. (1995) *Eur. J. Biochem.* 234, 443–451.
- [21] Sulkowski, E. (1985) *Trends Biotech. Sci.* 3, 1–7.
- [22] Matsushita, K., Ebisuya, H. and Adachi, O. (1992) *J. Biol. Chem.* 267, 24748–24753.
- [23] Lemma, E., Schägger, H. and Kröger, A. (1993) *Arch. Microbiol.* 159, 574–578.
- [24] Steinrück, P., Steffens, G.C.M., Pankus, G., Buse, G. and Ludwig, B. (1987) *Eur. J. Biochem.* 167, 431–439.
- [25] Tokunaga, M., Tokunaga, H. and Wu, H.C. (1982) *Proc. Natl. Acad. Sci. USA* 79, 2255–2259.
- [26] Weyer, K.A., Schäfer, W., Lottspeich, F. and Michel, H. (1987) *Biochemistry* 26, 2909–2914.
- [27] Stouthamer, A. (1992) *Antonie van Leeuwenhoek* 61, 1–33.
- [28] Welter, R., Gu, L.-Q., Yu, L. and Yu, C.-A. (1994) *J. Biol. Chem.* 269, 28834–28838.
- [29] Puustinen, A., Verkhovsky, M.I., Morgan, J.E., Belevich, N.P. and Wikström, M. (1996) *Proc. Natl. Acad. Sci. USA* 93, 1545–1548.
- [30] Blumberg, W.E. and Peisach, J. (1979) in *Cytochrome oxidase* (King, T.E., Orii, Y., Chance, B. and Okunuki, K., eds.), Elsevier, Amsterdam.
- [31] Iwata, S., Ostermeier, C., Ludwig, B. and Michel, H. (1995) *Nature* 376, 660–669.
- [32] Seelig, A., Ludwig, B., Seelig, J. and Schatz, G. (1981) *Biochim. Biophys. Acta* 636, 162–167.
- [33] Haltia, T., Finel, M., Harms, N., Nakari, T., Raitio, M., Wikström, M. and Saraste, M. (1989) *EMBO J.* 8, 3571–3579.
- [34] Myer, Y.P. (1971) *J. Biol. Chem.* 246, 1241–1248.
- [35] Cheesman, M.R., Greenwood, C. and Thomson, A.J. (1991) *Adv. Inorg. Chem.* 36, 201–255.
- [36] Carter, K. and Palmer, G. (1982) *J. Biol. Chem.* 257, 13507–13514.
- [37] Goldbeck, R.A., Einarsdottir, O., Daws, T.D., O'Connor, D.B., Surerus, K.K., Fee, J.A. and Kliger, D.S. (1992) *Biochemistry* 31, 9376–9387.